Pergamon

Chemical Engineering Science, Vol. 49, No. 24B, pp. 5681–5698, 1994

0009-2509/94 $7.00 + 0.00

0009–2509(94)00315-7

PRESSURE DROP AND LIQUID HOLDUP IN HIGH PRESSURE TRICKLE-BED REACTORS

MUTHANNA H. AL-DAHHAN* and MILORAD P. DUDUKOVIĆ
Chemical Reaction Engineering Laboratory, Chemical Engineering Department, Washington University, Campus Box 1198, One Brookings Drive, St Louis, MO 63130, U.S.A.

(*Received* 26 *May* 1994; *accepted for publication* 26 *September* 1994)

Abstract—The vast majority of commercial trickle-bed reactors, fixed bed of catalyst particles contacted by cocurrent downflow of gas and liquid, operate at high pressure. In this study Holub *et al.*'s (1992, 1993) phenomenological model has been extended to describe the effect of high pressure (i.e. increased gas density) on pressure drop and liquid holdup in the trickle flow regime. This model, based on annular two-phase flow in a slit, ties pressure drop and liquid holdup but was previously verified only at atmospheric pressure. The advantage of this model is that the Ergun constants E_1 and E_2, required by the model, are determined from single phase (gas) flow through the packing of interest and no two-phase flow data is needed. Experiments were conducted at high pressure over a range of gas and liquid velocities and different bed characteristics. The developed phenomenological analysis, describing the effect of high pressure and gas flow rate in terms of five limiting cases, matches well the experimental observations. The high pressure data collected in this study was used as a basis for comparing the prediction for pressure drop and liquid holdup of the model and of the available high pressure correlations. Holub *et al.*'s (1992) model matches experimental observations better than available correlations. It also predicts all trends in pressure drop and holdup correctly for all changes in operating variables such as pressure, liquid and gas superficial mass velocity and with physical properties of the gas and liquid.

1. INTRODUCTION

Trickle-bed reactors, fixed beds of catalyst particles contacted by cocurrent downflow of gas and liquid [Fig. 1(a)], are widely used in petroleum, petrochemical and chemical industries, pollution abatement, biochemical and electrochemical processing, etc. The vast majority of commercial trickle-beds operate at high pressure, up to about 20–30 MPa (3000–4500 psig), in order to improve the solubility of the gaseous reactant and/or achieve better heat transfer. Various flow regimes exist in a trickle-bed reactor depending on the superficial mass velocities, fluid properties and bed characteristics. Usually two broad regimes are classified: a low gas–liquid interaction regime, LIR, where gas–liquid shear does not affect the flow pattern; and a high gas–liquid interaction regime, HIR, where gas–liquid shear affects the flow pattern considerably. LIR includes the trickle flow regime which is also called gas continuous flow regime, while HIR includes pulse, spray, wavy, bubble, and dispersed bubble flow regimes. The design and scale-up parameters are affected differently in each flow regime as the hydrodynamics change from one regime to another. The choice of the particular regime depends on the nature of the reaction and the process conditions. In general, the trickle flow regime, the pulse flow regime, and the transition region between them are of particular interest in industry (Sato *et al.*, 1973; Charpentier and Favier, 1975; Midoux *et al.*, 1976; Chou *et al.*, 1977; Fukushima and Kusaka, 1977a,b, 1978, 1979; Talmor, 1977; Hofmann, 1978; Tosun, 1984; Levec *et al.*, 1986; Holub, 1990; Wammes and Westerterp, 1990).

A basic understanding of the hydrodynamics of trickle-bed reactors is essential to their design, scale-up, scale-down and performance. Liquid holdup and pressure drop are important hydrodynamic parameters for design and operation. Liquid holdup, which partially occupies the void volume of the packed bed, is a basic parameter for reactor design because it is related to other important parameters: the pressure gradient, gas–liquid interfacial area, the mean residence time of the liquid phase, catalyst loading per unit liquid volume, axial dispersion coefficient, and heat transfer coefficient at the wall, etc. Pressure drop represents the energy dissipated due to fluid flow through the reactor bed. It is important in determining the energy losses, the sizing of the compression equipment, liquid holdup, external contacting efficiency, gas–liquid interfacial area and mass transfer coefficients, etc. (Holub, 1990; Wammes *et al.*, 1991a,b; Al-Dahhan, 1993).

In contrast to the industrial trickle-bed reactors, which are usually operated at *high pressure*, most of the research reported in the literature concerning various aspects of trickle-bed reactors has been

*To whom correspondence should be addressed.

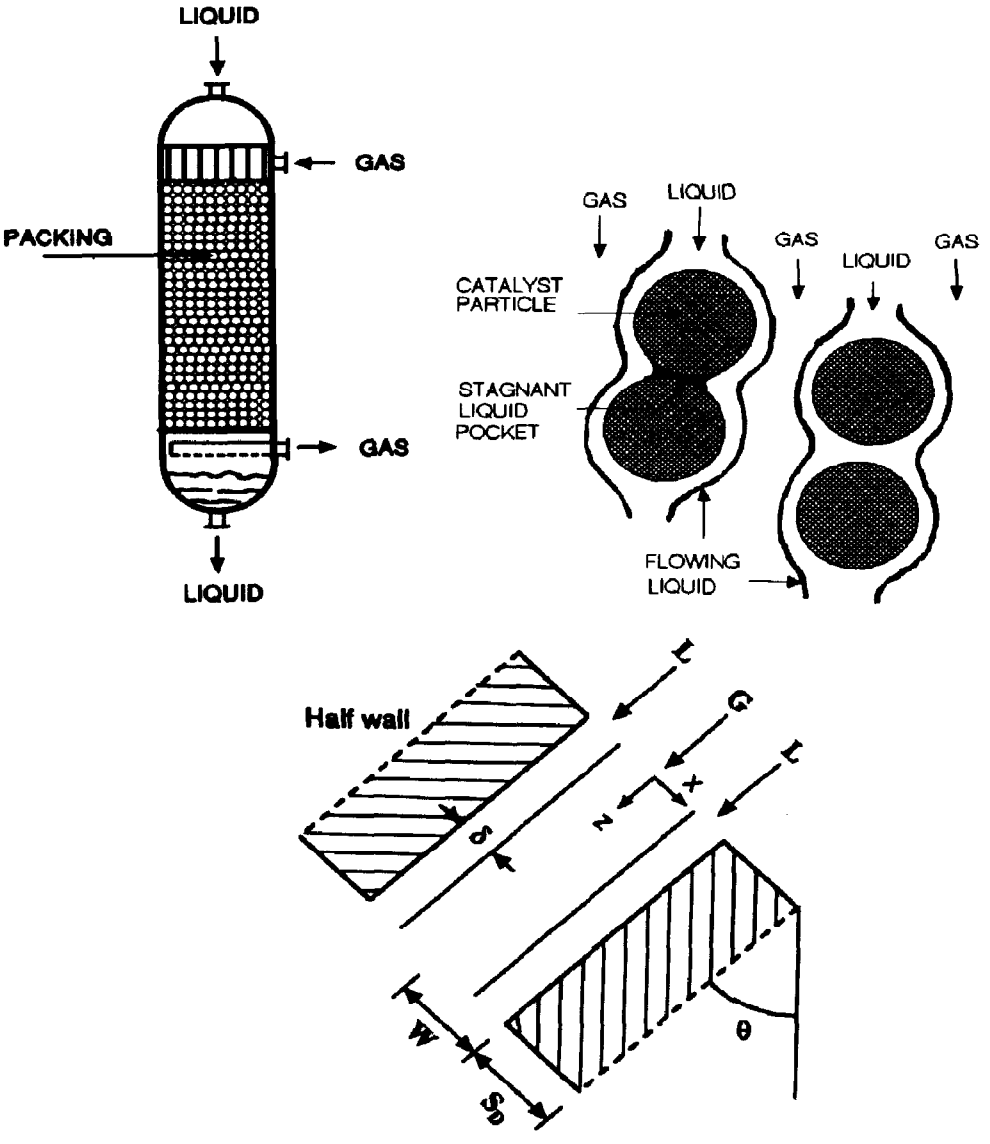

$$\frac{W}{S_D}=\frac{\varepsilon_B}{1-\varepsilon_B} \quad ; \quad \frac{\delta}{S_D}=\frac{\varepsilon_L}{1-\varepsilon_B} \quad ; \quad S_D=\frac{d_p}{6}$$

$$Cos\,\theta = T \quad ; \quad V_L=\left(\frac{U_L}{\varepsilon_L}\right)T \quad ; \quad V_G=\left(\frac{U_G}{\varepsilon_B}\right)T$$

Fig. 1. (a) Schematic diagram of a trickle-bed reactor. (b) Externally fully wetted particles in trickle-flow regime. (c) The geometry of a single slit (slit model of a trickle-bed).

performed at *atmospheric pressure*. High pressure data is scarce. Recently, few investigations concerned with liquid holdup and pressure drop in pressurized trickle-bed reactors have been reported (Wammes, 1990; Wammes *et al.*, 1990, 1991a,b; Larachi *et al.*, 1991a,b, 1992; Gianetto and Specchia, 1992; Marquez *et al.*, 1992). Their experimental observations show that at high pressure operation, for a given gas and liquid superficial velocity, liquid holdup decreases considerably while pressure drop increases significantly compared to low pressure operation. In these studies the developed correlations for prediction of pressure drop and liquid holdup are entirely empirical. Due to

complex interaction between the flowing phases and stationary packing, a quantitative description of two phase flow through a packed-bed based on fundamental principles has not yet been successfully achieved (Holub, 1990; Larachi *et al.*, 1991a,b, 1992; Wammes *et al.*, 1991a,b). In the absence of a fundamental approach, a phenomenological (or mechanistic) model or approach is preferred to strictly empirical correlations and often is very useful. A phenomenological model relies on building a simpler physical picture of the phenomena involved. Based on the simplified geometry, all pertinent equations are derived using the appropriate conservation laws and required accepted constitutive forms.

Holub (1990) and Holub *et al.* (1992, 1993) proposed a phenomenological model in the form of a modified Ergun equation, based on annular two phase flow in a slit, that tied pressure drop and holdup in trickle-flow regime. The model was verified only at *atmospheric pressure* and showed better agreement with liquid holdup and pressure drop data than previous models and correlations. The advantage of this model is that it does not depend on parameters determined by fitting two phase flow data since the Ergun constants E_1 and E_2 required by the model are determined from single (gas) flow through the packing of interest. Table 1 shows Holub *et al.*'s (1992) model as well as the recent proposed empirical correlations for prediction of pressure drop and liquid holdup at high pressure operation. The survey of the correlations and models for pressure drop and liquid holdup that were established based on atmospheric data can be found in many texts and articles (Shah, 1979; Ramachandran and Chaudhari, 1983; Dudukoviċ and Mills, 1986; Sai and Varma, 1987; Ellman *et al.*, 1988; Holub, 1990; Wammes, 1990; Zhukova *et al.*, 1990).

In the present study Holub *et al.*'s (1992) phenomenological lmodel has been extended to describe and incorporate the effect of high pressure (i.e. increased gas density) on pressure drop and liquid holdup in trickle flow regime. Experiments were conducted at high pressure over a range of gas and liquid velocities and different bed characteristics. The high pressure data obtained in this study is used to confirm the developed phenomenological analysis and as a basis for comparing the prediction for pressure drop and holdup of Holub *et al.*'s (1992) model and the available high pressure correlations (Table 1).

2. PHENOMENOLOGICAL ANALYSIS

In trickle-flow regime the liquid flows as films or rivulets over the catalyst bed, while the gas flows as continuous phase through the remaining voids as depicted in Fig. 1(b). Holub (1990) and Holub *et al.* (1992) represented the complex geometry of the actual void space in a packed bed of particles as a single, flat-walled slit of average half width, W, half wall thickness, S_D, and angle of inclination, θ, to the vertical axis as shown in Fig. 1(c). The liquid is assumed to completely wet the wall with a film of uniform thickness, δ, while the gas flows in the central core. This is clearly a very simple representation of the actual complex void geometry and flow in it. The slit parameters are related to that of the actual trickle-bed by the following assumptions: (i) the void to solid and liquid to solid volumetric ratios are assumed to be the same in the slit and the bed, (ii) the solid surface area per unit solid volume is the same in the two geometries (i.e. the slit and the bed), (iii) the average slit inclination is related to the bed tortuosity, T, (iv) the phase superficial velocities are the same in the slit and the actual bed. These assumptions lead to the relationships shown in Fig. 1(c). By using these relationships, two phase flow momentum balance equations in the slit model are mapped to the actual bed model which yields the dimensionless equations for the trickle flow regime in the form of modified Ergun equations (Table 1). E_1 and E_2 are the Ergun constants which characterize the bed [$E_1 = 72T^2$, $E_2 = 6Tf_{\text{wall cat.}}$ (Holub, 1990)] and are not two-phase flow parameters. Therefore, they are determined from single phase flow experiments in the bed of interest (e.g. gas phase flow in dry bed) as shown by Holub (1990). The equations of Holub's model form a closed system for determining the pressure drop and liquid holdup. By substituting eqs (1) and (2) into eq. (3) of Table 1, a nonlinear implicit equation for liquid holdup is obtained which can be readily solved numerically by Newton–Raphson method with only a few iterations. Knowing the liquid holdup, pressure drop can be evaluated by eq. (1) or (2) in Table 1. The validity of the model predictions was confirmed at atmospheric pressure operation. No attempt has been made to test it at conditions of interest which is high pressure operation.

By extending Holub's model to incorporate the effect of high pressure (i.e. the increased gas density), the influence of reactor pressure and gas flow rate on pressure drop and external liquid holdup in the trickle flow regime are explained phenomenologically as follows.

The energy dissipation in a gas–liquid cocurrent downflow packed bed reactor is due to the frictional losses at the packing surface and the driving forces acting on the liquid flow. The driving forces consist of the pressure gradient and the gravitational force. The pressure gradient depends on the velocity and on the density of the flowing fluids. Higher liquid/gas superficial velocity and/or gas density produce a higher pressure gradient while higher liquid density increases the gravitational force. Since the gas density depends on the gas pressure, increasing the reactor pressure makes the gas more dense. Therefore, the effect of the gas phase on pressure drop can be separated into the

Table 1. Recent correlations for pressure drop and liquid holdup (based on data obtained at high pressure) and Holub *et al.*'s model (Holub *et al.*, 1992)

Author	Packing type	d_p(cm)	d_t(cm)	ε_B	Pressure	Approach
Holub *et al.* (1992)	Glass beads	0.3	7.95	0.375	atm	Phenomenological
	Extrudate	0.16 × 0.32	2.54	0.335		
	Sphere alumina	0.32	12.22	0.45		

$$\psi_L = \left(\frac{\varepsilon_B}{\varepsilon_L}\right)^3 \left[\frac{E_1 Re_L}{Ga_L} + \frac{E_2 Re_L^2}{Ga_L}\right] \tag{1}$$

$$\psi_G = \left(\frac{\varepsilon_B}{\varepsilon_B - \varepsilon_L}\right)^3 \left[\frac{E_1 Re_G}{Ga_G} + \frac{E_2 Re_G^2}{Ga_G}\right] \tag{2}$$

$$\psi_L = 1 + \frac{\rho_G}{\rho_L}(\psi_G - 1) \tag{3}$$

where

$$\psi_\alpha = \frac{\Delta P/Z}{\rho_\alpha g} + 1, \ \alpha = L \text{ or } G$$

Wammes *et al.* (1991a,b)	Glass beads	0.3	5.1	0.39	Up to 7.5 MPa	Empirical
	Cyl. alumina	0.32 × 0.33		0.41		

$$\beta_d = 3.8\left(\frac{\rho_L U_L d_p}{\mu_L}\right)^{0.55}\left[\frac{d_p^3 \rho_L^2 g}{\mu_L^2}\left(1 + \frac{\Delta P/Z}{\rho_L g}\right)\right]^{-0.42}\left(\frac{6(1-\varepsilon_B)d_p}{\varepsilon_B}\right)^{0.65} \tag{4}$$

$$\frac{\Delta P}{0.5\rho_G U_G^2}\left(\frac{d_p}{Z}\right) = 155\left[\frac{\rho_G U_G d_p \varepsilon_B}{\mu_G(1-\varepsilon_B)}\right]^{-0.37}\left[\frac{1-\varepsilon_B}{\varepsilon_B(1-\beta_t)}\right] \tag{5}$$

Larachi *et al.* (1991a)	Glass beads	0.14–0.2	5	—	Up to 12 MPa	Empirical

$$\beta_t = 1 - 10^{-\Gamma} \tag{6}$$

$$\Gamma = 1.22\frac{We_L^{0.15}}{X_G^{0.15} Re_L^{0.2}} \tag{7}$$

$$\frac{(\Delta P/Z)d_h \rho_G}{2G^2} = \frac{1}{\{(Re_L We_L)^{0.25} X_G\}^{1.5}}\left[31.3 + \frac{17.3}{\{(Re_L We_L)^{0.25} X_G\}^{0.5}}\right] \tag{8}$$

where

$$X_G = \frac{G}{L}\sqrt{\frac{\rho_L}{\rho_G}}, \quad Re_L = \frac{\rho_L U_L d_p}{\mu_L}, \quad We_L = \frac{L^2 d_p}{\rho_L \sigma_L}, \quad d_h = \left[\frac{16\varepsilon_B^3}{9\pi(1-\varepsilon_B)^2}\right]^{0.33} d_p$$

Ellman *et al.* (1988, 1990)	Sphere and cylinder	0.116–0.3	2.3–10.0	0.27–0.49	Up to 10 Mpa	Empirical

$$\beta_d = 10^k \tag{9}$$

$$k = 0.001 - \frac{0.42}{\left[X_L^{0.5} Re_L^{-0.3}\left(\frac{a_s d_h}{(1-\varepsilon_B)}\right)^{0.3}\right]^{0.48}} \tag{10}$$

$$\frac{(\Delta P/Z)d_h \rho_G}{2G^2} = 200(X_G \delta_2)^{-1.2} + 85(X_G \delta_2)^{-0.5} \tag{11}$$

where

$$\delta_2 = \frac{Re_L^2}{(0.001 + Re_L^{1.5})}, \quad X_G = \frac{G}{L}\sqrt{\frac{\rho_L}{\rho_G}}, \quad X_L = \frac{1}{X_G}, \quad Re_L = \frac{\rho_L U_L d_p}{\mu_L},$$

$$a_s = \frac{6(1-\varepsilon_B)}{d_p}, \quad We_L = \frac{L^2 d_p}{\rho_L \sigma_L}, \quad We_G = \frac{G^2 d_p}{\rho_G \sigma_L}, \quad d_h = \left[\frac{16\varepsilon_B^3}{9\pi(1-\varepsilon_B)^2}\right]^{0.33} d_p$$

effect of the superficial gas velocity and the effect of the reactor pressure. Accordingly, an increase in the reactor pressure (at constant superficial gas and liquid velocities for a given liquid and gas phasse) results in a higher pressure drop over the packed bed due to the increase in the gas phase density. Increasing the superficial gas velocity at high pressure, yields an even much higher pressure drop across the bed.

Based on slit model, the dependence of liquid holdup on the pressure drop is described by the following equation (Al-Dahhan, 1993):

$$\varepsilon_L = \varepsilon_B \left[\frac{E_1 Re_L + E_2 Re_L^2}{Ga_L \left(1 + \frac{\Delta P/Z}{\rho_L g} \right)} \right]^{1/3} \quad (12)$$

where, the term $(\Delta P/Z)/(\rho_L g)$ is the dimensionless pressure drop which represents the ratio of the pressure drop to the gravitational forces.

In general, as liquid superficial flow rate increases, pressure drop increases as discussed above. The increase in the denominator of eq. (12), due to the increase in $(\Delta P/Z)/(\rho_L g)$, is smaller than the increase in the numerator due to the increase in Re_L and Re_L^2. Therefore, liquid holdup always increases as liquid flow rate increases. When higher liquid density is utilized, dimensional pressure drop and gravitational force increase. In this case, the dimensionless pressure drop, $(\Delta P/Z)/(\rho_L g)$, decreases while liquid holdup increases. Therefore, liquid holdup is affected both by $(\Delta P/Z)/(\rho_L g)$ and liquid physical properties (density and viscosity) which are accounted for in Re_L and Ga_L. The effect of bed characteristics on pressure drop and liquid holdup are considered in the Ergun constants, bed voidage, and Galileo number.

According to eq. (12), five limiting cases can be deduced for a given packed bed. These cases describe the effect of reactor pressure and gas flow rate on liquid holdup as well as on the dimensionless pressure drop.

- *Case 1: No gas flow*
  Without gas flow but with stagnant gas present in the system, i.e. $U_G = 0$ the ratio $(\Delta P/Z)/(\rho_L g)$ is zero. The gravitational force is the only driving force. Hence, liquid holdup is maximal. Although this case is not of practical interest, it is considered for completeness as a limiting case for low gas flow rates.
- *Case 2: low pressure, low gas superficial velocity*
  At atmospheric to low pressure and at low gas superficial velocity, the pressure drop is negligible in comparison to the gravitational force. Therefore, the dimensionless pressure drop, $(\Delta P/Z)/(\rho_L g)$, is small, changes only slightly with variation in gas velocity and can be neglected. Hence, the reactor pressure effect on liquid holdup is also negligible.
- *Case 3: low pressure, high gas superficial velocity*
  At atmospheric pressure to slightly elevated pressure and at high gas superficial velocity, the pressure gradient increases in comparison to the gravitational force. Thus, the ratio $(\Delta P/Z)/(\rho_L g)$ is larger which causes a decrease in liquid holdup. The gas phase superficial velocity now starts to influence liquid holdup. Moreover, the increase in pressure drop at high range of liquid flow rate is larger than that of *Case 2*. Hence, the quantitative difference in the numerator and the denominator of eq. (12) at higher liquid flow rate is greater than that at low liquid flow rate. The effect of gas velocity in this case is more noticeable at high liquid flow rate than that at low flow rate.
- *Case 4: High pressure, low gas superficial velocity*
  At elevated pressure the gas density increases. As a result the pressure drop increases. Thus, the ratio $(\Delta P/Z)/(\rho_L g)$ increases which causes a decrease in liquid holdup. Since the effect of gas velocity on pressure drop is greater than that of gas density (Ergun, 1952), the influence of elevated pressure at low gas velocity is less than that of *Case 3* at both low and high liquid flow rates.
- *Case 5: High pressure, high superficial gas velocity*
  At elevated pressure and high gas superficial velocity, the pressure drop increases significantly due to both gas density and superficial velocity. As a result, the dimensionless pressure drop, $(\Delta P/Z)/(\rho_L g)$, increases significantly and hence liquid holdup decreases considerably. Therefore, the effect of gas flow rate on pressure drop and liquid holdup is more pronounced at elevated pressure. Moreover, the effects of high pressure and high gas velocity at high liquid flow rate on pressure drop and liquid holdup are significantly greater than that at low liquid flow rate. In general, the effect in this case is noticeably larger than in all other cases discussed above.

3. EXPERIMENTAL INVESTIGATION

3.1. *Experimental facility*

High pressure trickle-bed facility has been designed and developed to operate at a pressure up to 7 MPa (~1000 psig) (Al-Dahhan, 1993). Figure 2 shows the process and instrumentation diagram of the facility. The facility consists of a high pressure trickle-bed reactor set-up, liquid and gas delivery systems, and data acquisition system. This facility allows low and high pressure experiments and measurements of liquid holdup and pressure drop simultaneously over a broad range of operating conditions. Two reactors have been designed and constructed. One contains a thick optically clear acrylic window (ID = 2.2 cm) to observe the two

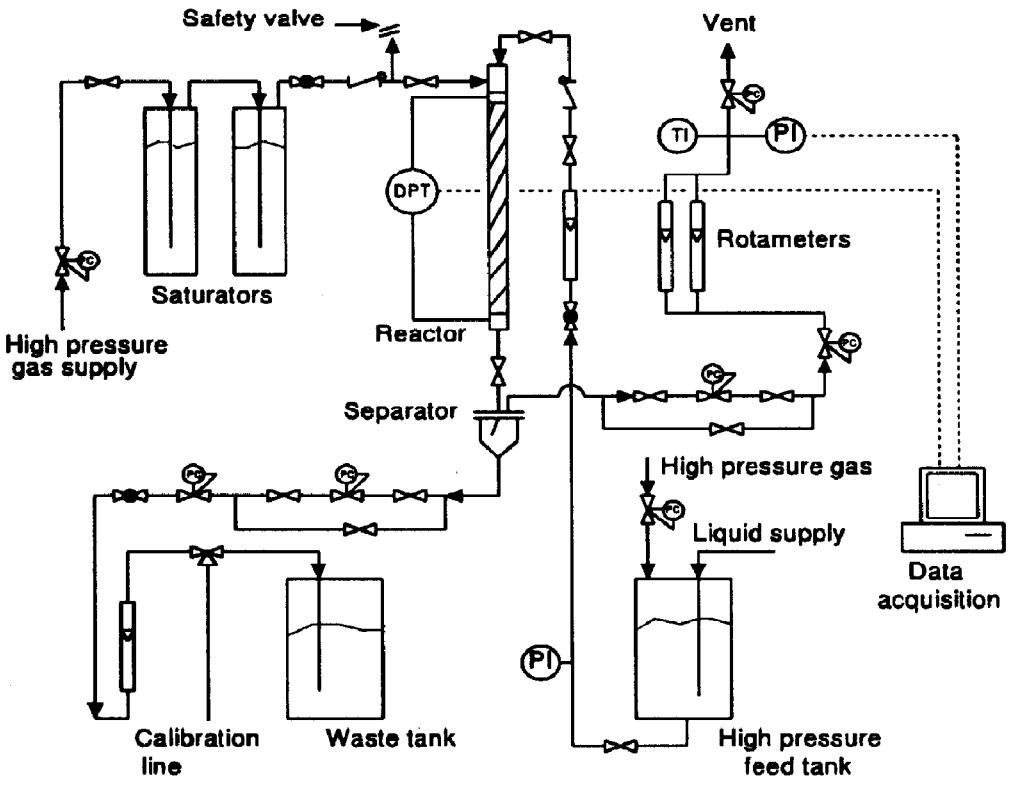

Fig. 2. Process and instrumentation diagram (P&ID) of the trickle-bed reactor facility.

phase flow at least near the wall while the other is 1 in. stainless-steel tubing (ID = 2.19 cm). The length of these reactors is 22.5 in. (57.15 cm). The reactor's gas–liquid distributor has been designed similar to the industrial type distributor to ensure uniform liquid and gas distribution at the bed inlet. The bottom of the reactor is connected to the gas–liquid separator. The separator is constructed from a thick optically clear acrylic to monitor the liquid level. A demister of stainless steel mesh is mounted in the upper part of the separator to trap the liquid mist from the gas effluent stream. Liquid phase is delivered to the reactor by high pressure feed tank. The exit liquid stream from the gas–liquid separator pass through back pressure regulators to the rotameter and then to the waste tank. The gas phase is delivered to the reactor from high pressure gas cylinders. The gas is allowed to pass through two high pressure saturators (bubblers) to be saturated with liquid in order to prevent evaporation in the reactor catalyst bed. The gas outlet stream from the gas/liquid separator passes through two back pressure regulators. Upon leaving the regulators, the gas flows to high and low range rotameter and then to the vent. Two high pressure differential pressure transducers (0–12.4 and 0–186 kPa) which are used to measure the pressure drop across the catalyst bed, are connected to the top and bottom of the reactor bed. Liquid holdup is measured by the draining method in which, by simultaneously shutting off the inlet and outlet streams and draining the reactor, draining holdup can be measured. The remaining holdup in the bed is measured by weighing the reactor after being drained and subtracting the weight of the dry reactor. This holdup consists of external to the catalyst and capillary (inside the pore) holdups.

The facility is connected to a portable, flexible and user friendly data acquisition and computation system. Detailed discussion about the design and the facility development can be found in Al-Dahhan (1993).

3.2. *Operating conditions investigated*

The flow conditions for the collected pressure drop and liquid holdup data were selected in the trickle flow regime. Figure 3 shows the trickle flow regime that is covered experimentally on the flow map of Fukushima and Kusaka (1977a,b) developed based on atmospheric data. However, at high pressure operation the trickle flow regime is extended since at elevated pressure this regime shifts toward higher liquid throughput (Wammes, 1990; Wammes and Westerterp, 1990; Al-Dahhan, 1993). Visual observation through the acrylic window and by stable and steady pressure drop

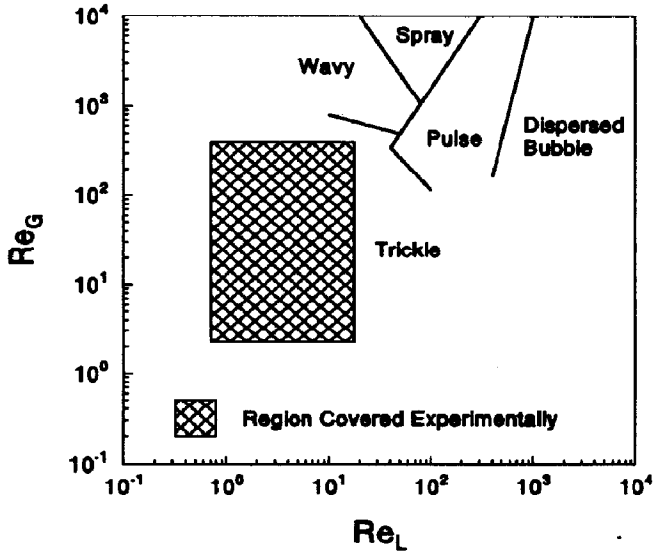

Fig. 3. Region of trickle flow regime covered experimentally in this study [flow map based on Fukushima and Kusaka (1977a,b)].

Table 2. Range of covered operating conditions

Condition	Covered range
Reactor pressure	
MPa	$0.31 \leq P \leq 5.0$
Psig	$30 \leq P \leq 700$
Gas superficial velocity, cm/s	$1 \leq U_G \leq 11.7$
Gas superficial mass velocity,k kg/m^2 s	$6.64 \times 10^{-3} \leq G \leq 4.03$
Liquid superficial velocity, cm/s	$239 \leq U_L \leq 1482$
Liquid superficial mass velocity, kg/m^2 s	$0.42 \leq L \leq 4.1$
Temperature, K	≈ 298

Table 3. Physical properties of liquid–gas systems at 298 K and 1 atm

System	Density (kg/m^3)	Viscosity (N s/m^2)	Surface tension (N/m)
Liquid phase			
Water	1000	1.0×10^{-3}	72×10^{-3}
Hexane	663	3.07×10^{-4}	18.4×10^{-3}
Gas phase			
Nitrogen	1.15	1.78×10^{-5}	—
Helium	0.166	1.97×10^{-5}	—

measurements also indicate that the operating regime is trickle flow.

The influence of reactor pressure and gas flow rate on pressure drop and liquid holdup are investigated experimentally over a range of gas–liquid velocities and different bed characteristics. The range of reactor pressure and liquid and gas superficial velocities covered are shown in Table 2. The physical properties of the gas–liquid system are listed in Table 3, while the packing bed characteristics utilized in this investigation are illustrated in Table 4. The reported Ergun constants, E_1 and E_2, were determined for each bed prior to the two phase flow experiments using gas flow only at three different reactor pressures (0.31, 1.03 and 2.07 MPa). The same values of the constants (within ±5%) were obtained at all these pressures.

Prior to each two phase flow experiment, the catalyst bed, after being extensively prewetted by soaking the bed and leaving it soaked overnight, is operated first in the high interaction regime (pulse and/or bubble flow regime) at high liquid mass velocities and then the mass velocities are reduced to the desired level at which wetting efficiency,

Table 4. Packed-bed characteristics

Reactor/Packing	Characteristics
Reactor	
Acrylic window reactor	d_r = 2.22 cm; length = 57.23 cm
Stainless-steel reactor	d_r = 2.19 cm; length = 57.31 5cm
Packing	
Glass beads–stainless-steel reactor	Type: nonporous sphere; d_p = 0.114 cm; d_r/d_p = 20; bed length (Z) = 51.71 cm; ε_B = 0.392; E_1 = 334.1; E_2 = 3.23
Silica shell–acrylic window reactor	Type: porous sphere; d_p = 0.152 cm; d_r/d_p = 14.6; bed length (Z) = 51.63 cm; ε_B = 0.412; ε_p = 0.697; E_1 = 260.2; E_2 = 2.48
0.5% Pd/alumina–stainless-steel reactor	Type: porous extrudate; size = (0.157 × 0.43) cm; $(d_p)_{eq}$ = 0.199 cm; d_r/d_p = 11; bed height (Z) = 51.61; ε_B = 0.355; ε_p = 0.599; E_1 = 218.0; E_2 = 1.89

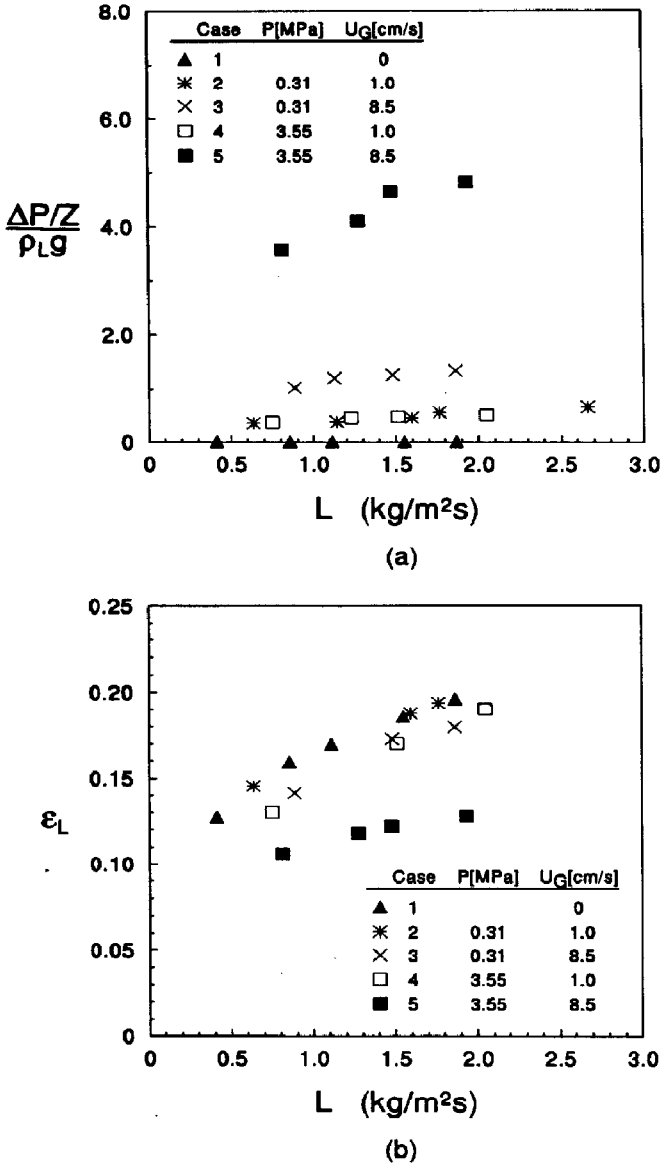

Fig. 4. Effect of reactor pressure and gas flow rate on pressure drop and liquid holdup. System: hexane/nitrogen; porous spherical silica shell; d_r/d_p = 14.6.

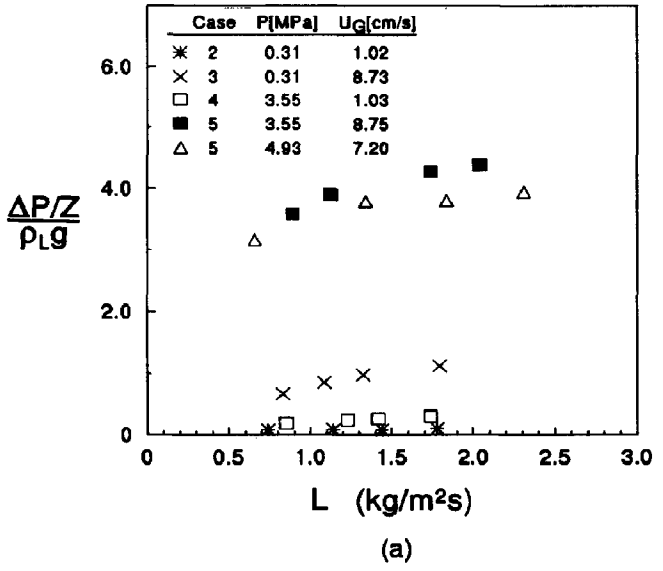

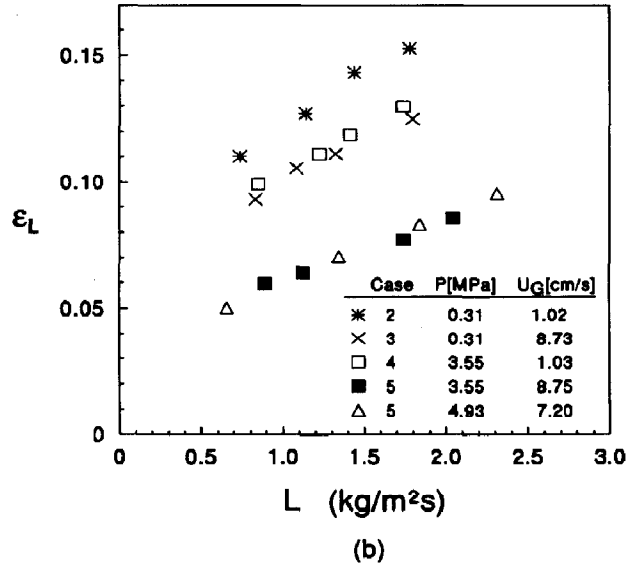

Fig. 5. Effect of reactor pressure and gas flow rate on pressure drop and liquid holdup. System: hexane/nitrogen; porous extrudate of 0.5% Pd on alumina; $d_r/d_p = 11$.

pressure drop and liquid holdup are measured. This procedure, besides assuring a uniform liquid–gas distribution at the bed entrance, minimizes liquid maldistribution and prevents hysteresis effects in measured pressure drop (Kan and Greenfield, 1979; Levec *et al.*, 1986; Dudukovič *et al.*, 1991). The operation is assumed to be stable where the data is taken when the reactor pressure, pressure drop and the gas and liquid throughput do not change for at least 5 min. The data are reproducible within less than ±5%.

4. RESULTS AND DATA ANALYSIS

Some of the experimental observations obtained in this study are illustrated in Figs 4–6. The phenomenological description of the influence of high pressure and gas flow rate on pressure drop and liquid holdup matches very well the experimental observations. The data clearly reveals the mechanistic cases discussed previously (cases 1–5). In case of trickle flow without gas flow (case 1), the pressure gradient is zero and liquid holdup is the highest as shown in Fig. 4. At low pressure

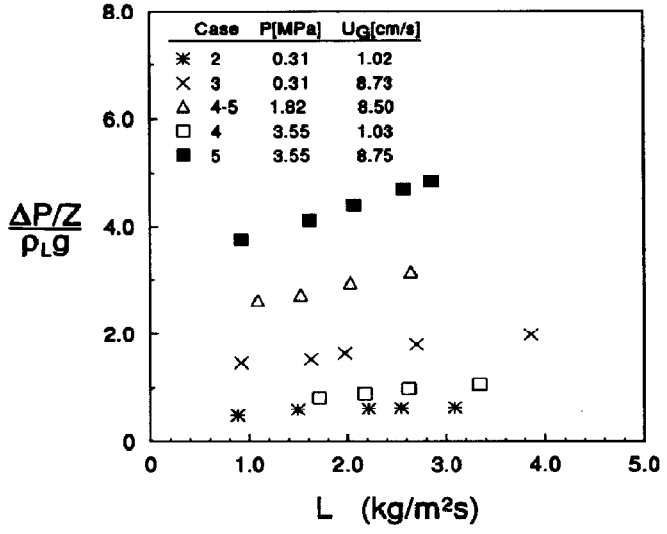

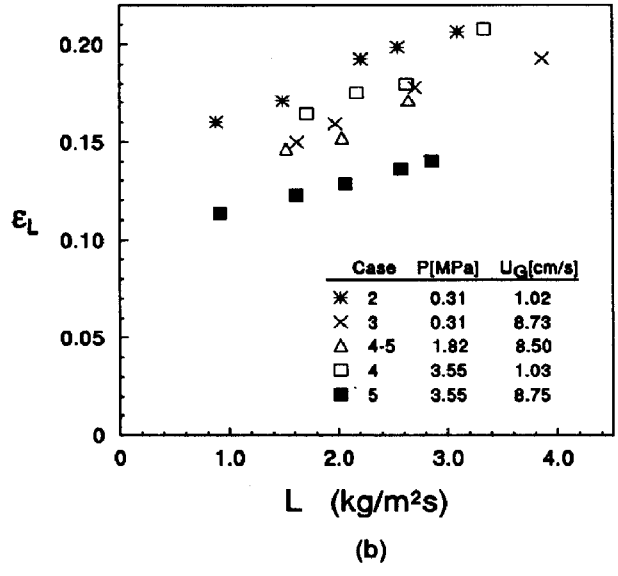

Fig. 6. Effect of reactor pressure and gas flow rate on pressure drop and liquid holdup. System: water/nitrogen; porous extrudate of 0.5% Pd on alumina; $d_r/d_p = 11$.

and low superficial gas flow rate (case 2), the dimensionless pressure drop increases slightly while liquid holdup does not decrease measurably compared to that of case 1 at the same liquid mass velocity. At fixed liquid mass velocity, as gas flow rate increases (case 3), the dimensionless pressure drop increases and liquid holdup decreases. At high pressure operation and low gas velocity (case 3), pressure drop increases slightly and liquid holdup decreases a little compared to the values at low pressure (case 2) at the same gas superficial velocity. At fixed liquid mass velocity, if the increase in the gas superficial velocity is the same in case 3 (low pressure and high gas flow rate) and in case 4 (high pressure and low gas flow rate), the effect on pressure drop in case 3 is larger than that in case 4 while the effect on holdup is about the same in both cases. At high pressure and high gas velocity (case 5), the dimensionless pressure drop increases significantly and liquid holdup decreases considerably. The effect of the operating conditions in this case is obviously much larger than in other cases.

Figures 5 and 6 confirm that the effect of gas flow rate on pressure drop and holdup is much more

pronounced at elevated pressure for all liquid mass velocities. For example, as shown in Fig. 5, the change in pressure drop and holdup at given liquid mass velocity is much larger when the gas superficial velocity is increased from 1.02 (cm/s) to 8.75 (cm/s) at 3.55 MPa than when the same increase in gas superficial velocity occurs at 0.31 MPa. Figure 6 demonstrates that at operating conditions between case 4 and 5, pressure drop and liquid holdup lie between case 3 and 5. It also shows that at constant gas superficial velocity (e.g. about 8.5 to 8.7 cm/s) and at constant liquid mass velocity, pressure drop increases and liquid holdup decreases as reactor pressure increases (e.g. compare data at 0.31 MPa, 1.82 MPa and 3.55 MPa). It is evident that the effects of reactor pressure and gas flow rate at high pressure on holdup and pressure drop are noticeable and need to be considered at operating conditions of industrial interest. It is noteworthy to mention that it is not conductive to improved understanding to describe such effects on pressure drop and liquid holdup by representing the data in terms of gas mass superficial velocity, as Larachi *et al.* (1991a) did. This is because within the gas mass superficial velocity the two effects of gas density (reactor pressure) and gas flow rate are then linked together while the magnitude of their separate contribution to the pressure drop and holdup depends on the range of pressure and gas flow rate as mentioned above (the effect of gas superficial velocity is much more pronounced at high pressure). For example, in Figs 4–6 the gas mass superficial velocity of case 4 (U_G = 1 cm/s, P = 3.55 MPa, ρ_G = 40.266 kg/m^3) is 0.415 kg/m^2 s while that of case 3 (U_G = 8.7 cm/s, P = 0.31 MPa, P_G = 3.497 kg/m^3) is 0.304 kg/m^2 s. The gas mass superficial velocity in case 4 is higher than in case 3 but pressure drop is higher and liquid holdup is lower in case 3 than in case 4. This indicates decreasing pressure drop and increasing holdup with increased gas mass velocity. In contrast, comparison of case 4 and case 5 in Figs 4–6 would indicate an increase in pressure drop and decrease in liquid holdup with an increase in gas mass velocity. Clearly, there is no trend of pressure drop and holdup with gas mass velocity.

To investigate the effect of gas density at constant superficial gas velocity, hexane–nitrogen–helium systems were used. Helium pressure about seven times higher than that of nitrogen yields helium density equal to nitrogen density. Figure 7 shows that both systems at the same gas density render about the same pressure drop and holdup at liquid mass velocity. This confirms that the effect of high pressure operation is due to the increase in the gas density. The effect of bed characteristics on pressure drop and liquid holdup is illustrated in Fig. 8. It is obvious that the small catalyst size results in high pressure drop and liquid holdup.

The effects of liquid physical properties (density and viscosity) on the pressure drop and liquid holdup are demonstrated by comparing Figs 5 and 6. As liquid density increases (from hexane to water), liquid holdup and dimensional pressure drop, $\Delta P/Z$, increase, while the dimensionless pressure drop, $(\Delta P/Z)/(\rho_L g)$, decreases.

All experimental data in Figs 4–8 show that pressure drop and liquid holdup increase with increasing liquid mass velocity as usually observed under atmospheric pressure. Moreover, the effect of pressure and gas flow rate is more pronounced at higher liquid flow rates.

5. COMPARISON OF THE MODEL AND AVAILABLE CORRELATIONS

The high pressure data obtained in this study was used as a basis for comparing the predictions for pressure drop and liquid holdup of Holub *et al.*'s model (1992) and the available high pressure correlations shown in Table 1. Such comparison in terms of mean relative errors (the average of the absolute difference between the experimental and the predicted values divided by the experimental value) is shown in Table 5. It is evident that Holub's model is somewhat more accurate than the available high pressure correlations. The reasons for this might be that as opposed to correlations Holub's model is based on a physical description of the phenomena and does not require any parameter from fitting of two phase flow data where liquid maldistribution, axial dispersion and wall effects could be encountered. The model requires the Ergun constants for each bed of interest to be determined from single phase flow pressure drop measurements. Since these constants represent the bed characteristics, they are reactor pressure independent as verified experimentally in this study. Hence, since the approach utilized in this work, based on Holub's model, requires characterization of the packing of interest via single-phase flow pressure drop measurements and is based on an albeit simple but physical model of the two phase flow situation, it is not surprising that it predicts pressure drop and holdup better than the available correlations which do not contain the data taken in this study in their data base. It is remarkable that these entirely empirical correlations do indeed predict holdup and pressure drop within a reasonable range.

The error in Holub's model prediction for pressure drop and liquid holdup at high pressure operation in the beds of d_r/d_p = 11, 14.6 and 20 is bounded within the same range reported by Holub *et al.* (1993) at atmospheric pressure which is ±60% for pressure drop and ±20% for liquid holdup (Al-Dahhan, 1993). However, model prediction for pressure drop and liquid holdup improves for the bed of d_r/d_p = 20, as shown in Fig. 9, where the mean relative errors in pressure drop and holdup are 29% and 6.8%, respectively. This is because in a bed of $d_r/d_p \geq 20$, the liquid phase is better distributed than in a bed of $d_r/d_p < 20$ where

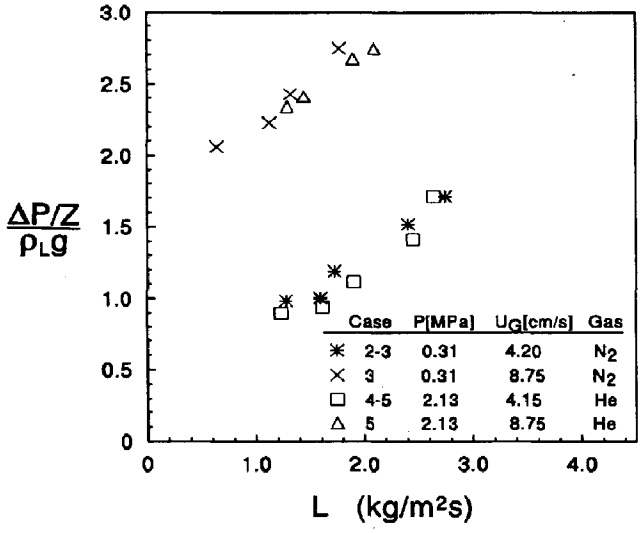

(a)

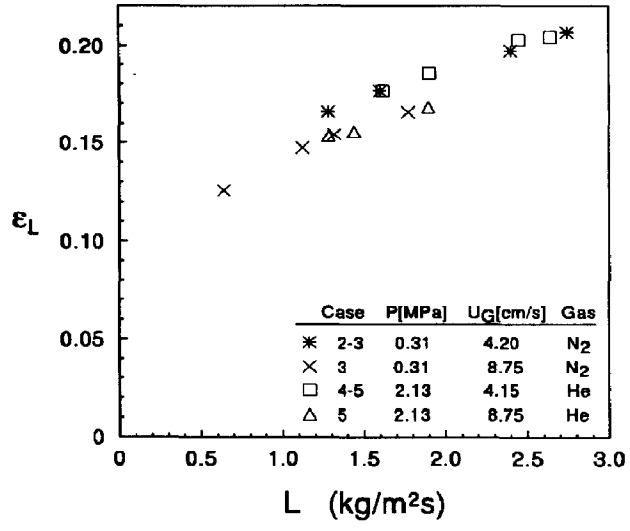

(b)

Fig. 7. Effect of gas density on pressure drop and liquid holdup. System: hexane/nitrogen and helium; nonporous spherical glass beads; $d_t/d_p = 20$.

Table 5. Comparison of models to data in terms of mean relative error (%)†

Model	Only high pressure data		All data of which 63% is high pressure	
	$\hat{e}_{(\Delta P/Z)/\rho_L g}$	$\hat{e}_{\varepsilon_L}$	$\hat{e}_{(\Delta P/Z)/\rho_L g}$	$\hat{e}_{\varepsilon_L}$
Holub (1990)	41	12	40	9.7
Wammes *et al.* (1991)	85	52	88	41
Larachi *et al.* (1991)	64	18	89	14.5
Ellman *et al.* (1988, 1990)	59	18	65	21.5

†Where $\hat{e} = \dfrac{\sum_{1}^{n} \dfrac{|\text{experimental value} - \text{predicted value}|}{\text{experimental value}}}{n}$

(n is the total number of data points).

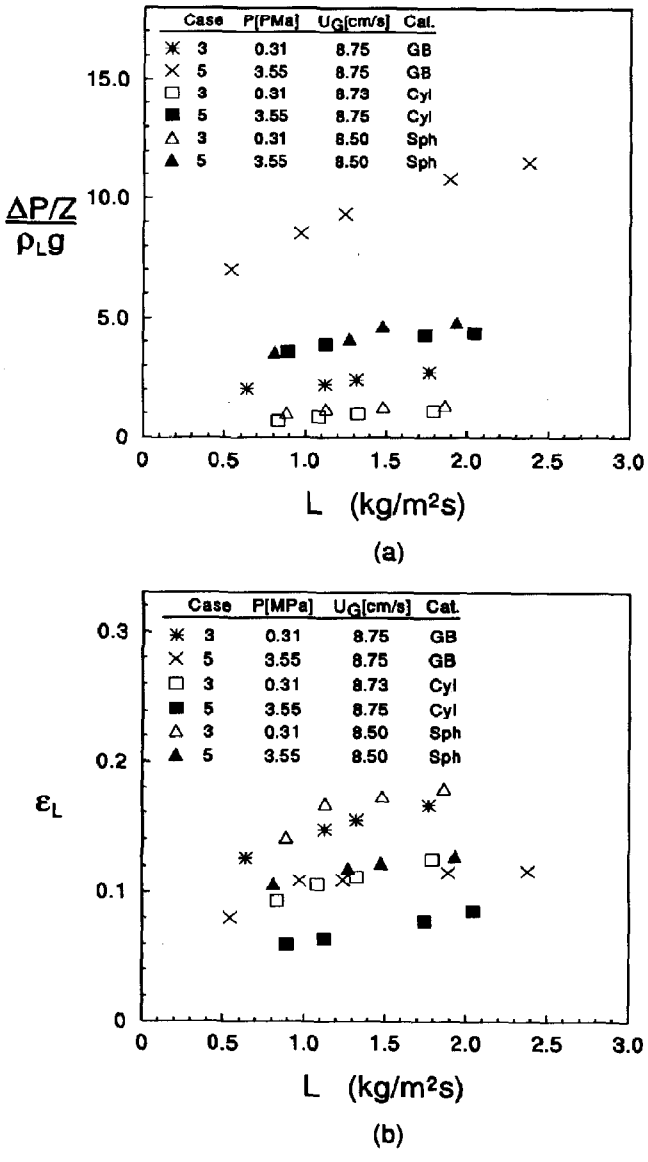

Fig. 8. Effect of bed characteristics on pressure drop and liquid holdup. System: hexane/nitrogen; GB: glass beads (d_p = 0.114 cm); Cyl: extrudate [$(d_p)_{eq}$ = 0.199 cm] Sph: spherical silica shell (d_p = 0.152 cm).

in the later bed wall effect, axial dispersion and liquid maldistribution are encountered (Dudukovic and Mills, 1986).

Based on the above, it is claimed that Holub *et al.*'s (1993) model predicts properly the trend of the effects of reactor pressure, gas flow rate, liquid flow rate, physical properties, and bed characteristics as demonstrated in Figs 4–8. The effect of the fluid physical properties (density and viscosity) are accounted for by the model's dimensionless groups, while the effects of bed characteristics are accounted for by the Ergun constants, bed voidage, and Galileo number. For example, when using low pressure nitrogen and helium at sufficiently high pressure to equal the density of nitrogen, the relative difference between the model predictions for pressure drop is within 6% caused by the difference in viscosity. This is well within the error of the model. This difference due to viscosity decreases as the pressure increases where the gas density effect dominates (Al-Dahhan, 1993).

Figure 10 illustrates the comparison of Holub *et al.*'s model prediction for pressure drop and holdup and experimental observations as a function of liquid mass velocity. The agreement between the model and data is very good at lower pressure and

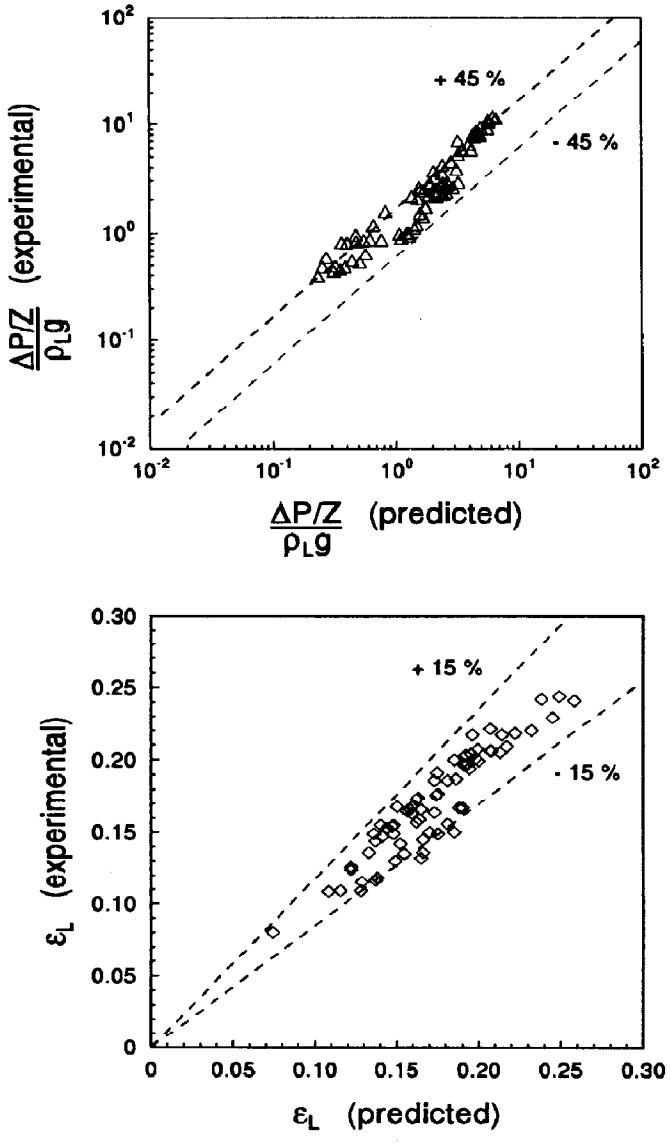

Fig. 9. Comparison of Holub's model (Holub, 1990) prediction and high pressure data obtained in the bed of $d_t/d_p = 20$.

over the range of liquid mass velocity at all levels of gas velocity. At high pressure the model consistently underpredicts the data. This is not unexpected. In the detailed derivation of the governing equations for the model Holub *et al.* (1993) neglected the interaction at the gas–liquid interface and assumed a discontinuity in both shear and velocity at the interface. Essentially zero velocity gradient and no shear are assumed at the free liquid film surface. It is well known, and documented by discussion in this study of cases 1 to 5, that this is not the case at high pressure. The original model equations [see Holub *et al.* (1993)] allow for gas–liquid interaction at the interface through parameters f_s (which relates gas and liquid shear stress at the interface) and f_v (which relates the gas and liquid velocity at the interface) and in the present model these parameters are taken as zero. Nonzero values are expected, based on physical arguments, to bring model predictions in closer agreement with data but that was not explored in this work due to a limited data base available, since a correlation of f_s and f_v with operating conditions would most likely be needed. A detailed discussion of Holub *et al.*'s (1992) model regarding the model error, identification of the most influential sources of errors and possibilities for further improvement can be found elsewhere (Holub, 1990; Holub *et al.*, 1993).

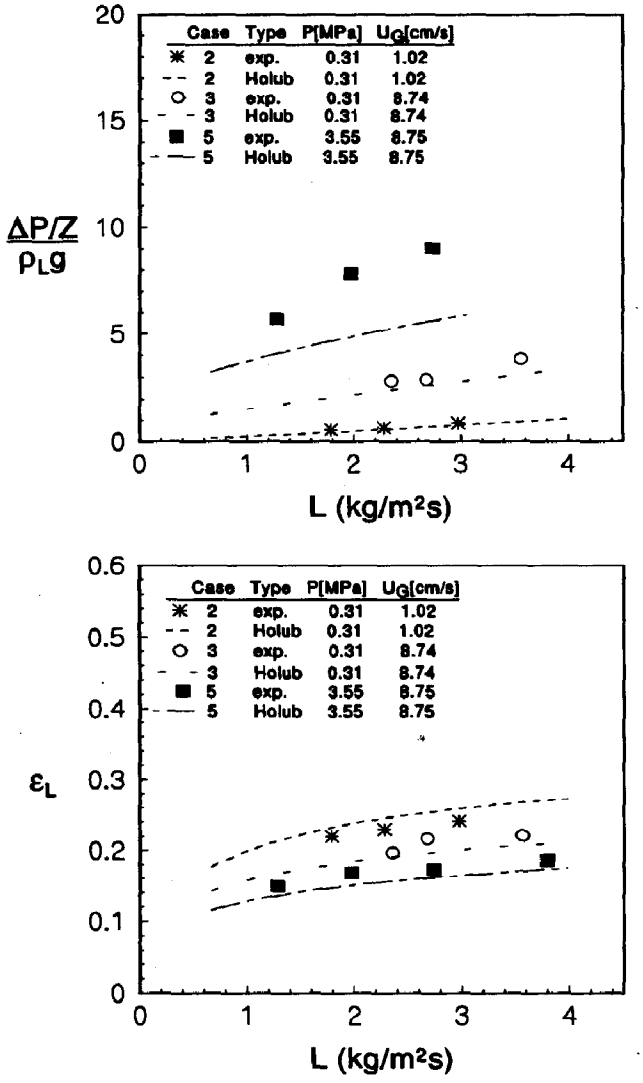

Fig. 10. Trend of Holub's model (Holub, 1990) prediction versus the experimental observation. System: water/nitrogen; nonporous glass beads; $d_r/d_p = 20$. The maximum relative error (the absolute difference between experimental and predicted values over the experimental value) in liquid holdup is 10% while in pressure drop is 38%.

Table 6 compares the deviations of predicted values for pressure drop and liquid holdup by various correlations and of the Holub *et al.*'s model at a selected set of conditions corresponding to cases 1–5. Examination of these values reveals that the error of the previous correlations exhibits no trend or pattern with the operating conditions while Holub *et al.*'s model does. Table 6 shows that as already mentioned Holub *et al.*'s model predictions at low pressure are better than at high pressure and that the error increases at high pressure with increased gas velocity, i.e. when the interactions between phases increase which are currently not accounted for in the present simplest form of the model. This, based on our discussion above, indicates the potential for further improvement in Holub *et al.*'s model by making it fit better in the high pressure–high gas flow rate regime. The scatter in the error of various correlations with operating conditions and no clear pattern either pressure or gas velocity seems to indicate that predictions of these correlations cannot be further improved. One should note, however, that the correlations cover a much broader flow regime than investigated in this study.

6. CONCLUSION

A phenomenological analysis in terms of five limited cases describes properly the experimental observations obtained in this study for the effects of

Table 6. Comparison of the deviations (%) of predicted values for pressure drop and liquid holdup at a selected set of conditions (glass beads bed and hexane–nitrogen system)†

	Larachi *et al.* (1991a)		Wammes *et al.* (1991a,b)		Ellman *et al.* (1988, 1990)		Holub *et al.* (1992)	
	$\hat{e}_{(\Delta P/Z)/\rho_L g}$	$\hat{e}_{\varepsilon_L}$	$\hat{e}_{(\Delta P/Z)/\rho_L g}$	$\hat{e}_{\varepsilon_L}$	$\hat{e}_{(\Delta P/Z)/\rho_L g}$	$\hat{e}_{\varepsilon_L}$	$\hat{e}_{(\Delta P/Z)/\rho_L g}$	$\hat{e}_{\varepsilon_L}$
Case 2								
U_G: 1.02 cm/s	200	4	97	8	83	32	23	2
P: 0.31 MPa								
Case 3								
U_G: 8.75 cm/s	11	4	86	32	66	11	18	4
P: 0.31 MPa								
Case 4								
U_G: 1.02 cm/s	133	13	93	20	90	44	42	8
P: 3.55 MPa								
Case 5								
U_G: 8.75 cm/s	66	19	85	116	57	40	48	9
P: 3.55 MPa								

†Where $\hat{e} = \dfrac{\sum_1^n \dfrac{|\text{experimental value} - \text{predicted value}|}{\text{experimental value}}}{n}$

(n is the total number of data points).

elevated pressure and gas flow rate on pressure drop and liquid holdup in trickle beds. According to this analysis the operating conditions can be represented by five distinct cases.

Holub *et al.*'s (1992) model predicts pressure drop and liquid holdup at high pressure somewhat better than the recently reported high pressure empirical correlations with mean relative error for pressure drop of 40% and for liquid holdup of 9.7%. Error is bounded by ±60% for pressure drop and by ±20% for holdup. Besides being based on a simple phenomenological approach it is the only model that does not contain any parameters fitted to two phase flow data where wall effects, axial dispersion and liquid maldistribution can be encountered. This model could be implemented in scale-up, scale-down and design as preliminary results (Al-Dahhan, 1993) indicate that Ergun constants are independent of reactor diameter, height and pressure.

According to the findings of this study, the other design, scale-up and operating parameters, such as flow regimes transition, liquid distribution, liquid–solid contacting efficiency, volumetric mass transfer coefficients, heat transfer, etc. need to be re-evaluated at high pressure operation before implementing models or correlations developed at atmospheric pressure.

Acknowledgement—The authors would like to acknowledge the support provided by the industrial sponsors of the Chemical Reaction Engineering Laboratory (CREL).

NOTATION

a_S total particles surface area per unit reactor volume, cm²/cm³

d_p particle diameter of the spherical particle, cm

$(d_p)_{eq}$ equivalent diameter of the cylindrical particle, cm

d_r reactor diameter, cm

E_1, E_2 Ergun constants

$f_{wall\ cat.}$ catalyst wall friction factor

g gravitational acceleration, cm/s²

G superficial gas mass velocity, kg/m² s

Ga_L dimensionless liquid Galileo number, $d_p^3\rho_L^2 g\varepsilon_B^3/\mu_L^2(1-\varepsilon_B)^3$

Ga_G dimensionless gas Galileo number, $d_p^3\rho_L^2 g\varepsilon_B^3/\mu_G^2(1-\varepsilon_B)^3$

h_d hydraulic diameter, cm

L superficial liquid mass velocity, kg/m² s

P operating pressure, MPa

$\Delta P/Z$ pressure drop per unit bed length, g/cm² s²

Re_L dimensionless liquid Reynolds number, $U_L\rho_L d_p/\mu_L(1-\varepsilon_B)$

Re_G dimensionless gas Reynolds number, $U_G\rho_G d_p/\mu_G(1-\varepsilon_B)$

S_D half wall thickness

T tortuosity

U_G superficial gas velocity, cm/s

U_L superficial liquid velocity, cm/s

V_G gas velocity in the slit, the interstitial gas velocity, cm/s

V_L liquid velocity in the slit, the interstitial liquid velocity, cm/s

W average half width of the slit model, cm

We_L dimensionless liquid Weber number, $U_L^2 d_p\rho_L/\sigma_L$

We_G dimensionless gas Weber number, $U_G^2 d_p\rho_G/\sigma_L$

X_G modified Lockart–Martinelli parameter

Z packed-bed length, cm

Greek letters

β_d, ω_d dynamic liquid saturation (liquid volume per void volume)
β_t total liquid saturation
δ liquid mean film thickness, cm
ε_B packed-bed void per reactor volume (bed porosity)
ε_L external liquid holdup per reactor bed volume ($\varepsilon_{Ld} + \varepsilon_{Ls}$)
ε_{Ld} dynamic liquid holdup per reactor volume
ε_{Ls} static liquid holdup per reactor volume
ε_P particle porosity
θ inclination angle of the slit, degree
μ_G gas viscosity, g/cm s
μ_L liquid viscosity, g/cm s
ρ_L liquid density, g/cm^3
ρ_G gas density, g/cm^3
σ surface tension, dyne/cm
ψ_G gas dimensionless pressure drop $[(\Delta P/Z)/(\rho_G g) + 1]$
ψ_L liquid dimensionless pressure drop $[(\Delta P/Z)/(\rho_L g) + 1]$

REFERENCES

Al-Dahhan, M., 1993, Effects of high pressure and fines on the hydrodynamics of trickle-bed reactors, D.Sc. Thesis, Washington University, St Louis, MO.

Charpentier, J. C. and Favier, M., 1975, Some liquid holdup experimental data in trickle bed reactors for foaming and nonfoaming hydrocarbons. *A.I.Ch.E. J.* **21**, 1213.

Chou, T. S., Worley Jr., F. L. and Luss, D., 1977, Transition to pulsed flow in mixed-phase cocurrent downflow through a fixed bed. *Int. Engng Chem. Process. Des. Dev.* **16**, 424.

Dudković, M. P. and Mills, P. L., 1986, Contacting and hydrodynamics in trickle-bed reactors, in *Encyclopedia of Fluid Mechanics* (Edited by N. P. Cheremisinoff), p. 969. Gulf Pub. Co.

Dudoković, M. P., Devanathan, N. and Holub, R., 1991, Multiphase reactors: Models and experimental verification. *Revue De L'Institut Francais–Du Petrole* **46**, 4.

Ellman, M. J., Midoux, N., Laurent, A. and Charpenteir, J. C. 1988, A new improved pressure drop correlation for trickle-bed reactors. *Chem. Engng Sci.* **43**, 2201.

Ellman, M. J., Midoux, N., Wild, G., Laurent, A. and Charpentier, J. C., 1990, A new improved liquid hold-up correlation for trickle-bed reactors. *Chem. Engng Sci.* **45**(7), 1677.

Ergun, S., 1952, Fluid flow through packed columns. *Chem. Engng Prog.* **48**, 89.

Fukushima, S. and Kusaka, K., 1977a, Interfacial area and boundary of hydrodynamic flow region in packed column with cocurrent downward flow. *J. Chem. Engng Japan* **10**(6), 461.

Fukushima, S. and Kusaka, K., 1977b, Liquid phase volumetric and mass transfer coefficient, and boundary of hydrodynamic flow region in packed volume with cocurrent downward flow. *J. Chem. Engng Japan* **10**(6), 468.

Fukushima, S. and Kusaka, K., 1978, Boundary of hydrodynamic flow region and gas-phase mass transfer coefficient in packed column with cocurrent downward flow. *J. Chem. Engng Japan* **11**(3), 241.

Fukushima, S. and Kusaka, K., 1979, Gas–liquid mass transfer and hydrodynamics flow region in packed columns with cocurrent upward flow. *J. Chem. Engng Japan* **12**(4), 296.

Gianetto, A. and Specchia, V., 1992, Trickle-bed reactors: state of art and perspectives. *Chem. Engng Sci.* **47**(13/14), 3197.

Hofmann, H. P., 1978, Multiphase catalytic packed-bed reactors. *Catal. Rev. Sci. Engng* **17**(21), 71.

Holub, R., 1990, Hydrodynamics of trickle bed reactors. D.Sc. Thesis, Washington University, St Louis, MO.

Holub, R. A., Duduković, M. P. and Ramachandran, P. A., 1992, A phenomenological model of pressure drop, liquid holdup and flow regime transition in gas–liquid trickle flow. *Chem. Engng Sci.* **47**(9/11), 2343.

Holub, R. A., Duduković, M. P. and Ramachandran, P. A., 1993, Pressure drop, liquid holdup, and flow regime transiton in trickle flow. *A.I.Ch.E. J.* **39**(2), 302.

Kan, K. and Greenfield, P. E., 1979, Pressure drop and holdup in two-phase cocurrent trickle flows through beds of small packings. *Ind. Engng Chem. Process Des. Dev.* **18**, 740.

Larachi, F., Laurent, A., Midoux, N. and Wild, G., 1991a, Experimental study of a trickle-bed reactor operating at high pressure: Two-phase pressure drop and liquid saturation. *Chem. Engng Sci.* **46**(5–6), 1233.

Larachi, F., Laurent, A., Wild, G. and Midoux, N., 1991b, Some experimental liquid saturation results in fixed-bed reactors operated under elevated pressure in cocurrent upflow and downflow of the gas and liquid. *Ind. Engng Chem. Res.* **30**, 2404.

Larachi, F., Laurent, A., Wild, G. and Midoux, N., 1992, Pressure effect on gas–liquid interfacial areas in cocurrent trickle-flow reactor. *Chem. Engng Sci.* **47**(9/11), 2325.

Levec, J., Saez, A. E. and Carbonell, R. G., 1986, Hydrodynamics of trickling flow in packed beds. *A.I.Ch.E. J.* **32**(3), 369.

Marquez, A. L., Larachi, F., Wild, G. and Laurent, A., 1992, Mass transfer characteristics of fixed beds with cocurrent upflow and downflow. A special reference to the effect of pressure. *Chem. Engng Sci.* **47**(13/14), 3485.

Midoux, M., Favier, M. and Charpentier, J. C., 1976, Flow pattern, pressure loss and liquid holdup data in gas–liquid downflow packed beds with foaming and nonfoaming hydrocarbon. *J. Chem. Engng Japan* **9**, 350.

Ramachandran, P. A. and Chaudhari, R. V., 1983, *Three Phase Catalytic Reaction*. Gordon and Breach Science Publishers, New York.

Sai, P. S. T. and Varma, Y. G. B., 1987, Pressure drop in gas–liquid downflow through packed beds. *A.I.Ch.E. J.* **33**, 2027.

Sato, Y., Hirose, T., Takahashi, F. and Toda, M., 1973, Pressure loss and liquid holdup in packed bed reactor with cocurrent gas–liquid downflow. *J. Chem. Engng Japan* **6**, 147.

Shah, Y. T., 1979, *Gas–Liquid–Solid Reactor Design*. McGraw Hill, New York.

Talmor, E., 1977, Two-phase downflow through catalyst beds. I: Flow maps, *A.I.Ch.E. J.* **22**, 868.

Tosun, G., 1984, A study of co-current downflow of nonfoaming gas–liquid systems in packed bed. I: Flow regimes; search for a generalized flow map. II: Pressure drop; search for a correlation. *Ind. Engng Chem. Process. Des. Dev.* **23**, 79.

Wammes, W. J. A., 1990, Hydrodynamics in cocurrent gas–liquid trickle-bed reactor at elevated pressure. Ph.D. Thesis, University of Twente, Enschede, Netherlands.

Wammes, W. J. and Westerterp, K. R., 1990, The influence of the reactor pressure on the hydrodynamics in a cocurrent gas–liquid trickle-bed. *Chem. Engng Sci.* **45**(8), 2247.

Wammes, W. J. A., Mechielsen, S. J. and Westerterp,

K. R., 1990, The transition between flow and pulse flow in a cocurrent gas–liquid trickle-bed reactor at elevated pressures. *Chem. Engng Sci.* **45**, 3149.

Wammes, W. J. A., Mechielsen, S. J. and Westerterp, K. R., 1991a, The influence of pressure on the liquid hold-up in a cocurrent gas–liquid trickle-bed reactor operating at low gas velocities. *Chem. Engng Sci.* **46**, 409.

Wammes, W. J. A., Middelkamp, J., Hulsman, W. J., deBaas, C. M. and Westerterp, K. R., 1991b, Hydrodynamics in a cocurrent gas–liquid trickle bed at elevated pressures. *A.I.Ch.E. J.* **37**(12), 1849.

Zhukova, T., Pisarenko, B. V. N. and Kafarov, V. V., 1990, Modeling and design of industrial reactors with a stationary bed of catalyst and two-phase gas–liquid flow—A review. *Int. Chem. Engng* **30**(1), 57.